J. Mol. Biol. (1981) **145**, 713–734

Genetic Analysis of the Histidine Operon Control Region of *Salmonella typhimurium*

H. Mark Johnston†

AND

John R. Roth

Department of Biology
University of Utah
Salt Lake City, Utah 84112, U.S.A.

(Received 10 July 1980)

Mutants of the histidine operon control region (*hisO*) include two classes: (1) those completely unable to express the operon (His auxotrophs), and (2) prototrophs that are unable to achieve fully induced levels of operon expression (still His^+ but sensitive to the drug amino-triazole). Using new, as well as previously existing *hisO* mutants, we constructed a fine-structure deletion map of *hisO*. Mutations that presumably alter the *his* promoter map at one end of *hisO*; mutations that alter the *his* attenuator map at the other end of *hisO*. Between the promoter and the attenuator lie a number of mutations that affect either the translation of the *his* leader peptide gene, or the formation and stability of *his* leader messenger RNA structures. All of the point mutations mapping in this central region revert to His^+ at a very high frequency (10^{-5} to 10^{-6}); this frequency is increased by both base substitution and frameshift-inducing mutagens. Many of the His^- mutants are suppressed by informational suppressors; all three types of nonsense mutations have been identified, demonstrating that translation of a region of *hisO* between the promoter and attenuator is essential for *his* operon expression. All of the *hisO* mutations tested are *cis*-dominant.

1. Introduction

The histidine operon of *Salmonella typhimurium* appears to be regulated without the mediation of any operon-specific regulatory protein. Despite intensive genetic analysis, no gene coding for a repressor or activator protein has been identified (Roth *et al.*, 1966; reviewed by Brenner & Ames, 1971). The regulation of this operon seems to be due entirely to features intrinsic to the *his* operon control region, *hisO*. The control region contains three sites important to operon regulation: the promotor (Ames *et al.*, 1963); the attenuator, where transcription of the *his* leader messenger RNA is terminated (Kasai, 1974); and, between these two

† Present address: Department of Biochemistry, Stanford University Medical School, Palo Alto, Calif. 94305, U.S.A.

0022-2836/81/040713-22 $02.00/0

sites, the *his* leader peptide gene (Barnes, 1978; DiNocera *et al.*, 1978). The leader peptide gene encodes a small polypeptide of 16 amino acids containing seven histidine residues in tandem (Barnes, 1978; DiNocera *et al.*, 1978).

Recently, we proposed a model for *his* operon regulation that involves the regulated formation of alternative stem-loop structures in the *his* leader mRNA (Johnston *et al.*, 1980). Depending on which of these alternative stem-loop structures forms, transcription either terminates at the attenuator, or proceeds across this site into the *his* structural genes. The position of a ribosome translating the *his* leader peptide gene, which is affected by the levels of histidyl-tRNA in the cell, determines which of the alternative conformations the *his* leader message assumes. Similar models that account for the regulation of other amino acid biosynthetic operons in bacteria have recently been proposed (Oxender *et al.*, 1979; Keller & Calvo, 1979). Our model is supported by the properties of a large number of mutants having alterations of the *his* operon control region. In this paper we describe the isolation and genetic characterization of these mutants.

Genetic studies that led to a detailed understanding of regulation of the *lac* operon relied heavily on the characterization of mutants with constitutive operon expression (Jacob & Monod, 1961). However, for the *his* operon, five of the six classes of mutants constitutive for *his* operon expression seem to have defects in the synthesis or processing of histidyl-tRNA; only one class, those having defects of the control region (*hisO*), affect the regulatory mechanism (Roth *et al.*, 1966; Roth & Ames, 1966; Silbert *et al.*, 1966; Singer *et al.*, 1972; Brenchly & Ingraham, 1973; Bossi & Cortese, 1977). To gain a better understanding of *his* operon regulation, we sought mutants of the control region exhibiting reduced operon expression. These mutants have provided much of the information on which our model is based.

Previously, very few *hisO* mutants exhibiting reduced operon expression existed. This was because the available selection methods chiefly yielded mutations in the nine *his* structural genes. Among these mutants, *hisO* types are rare (Fink *et al.*, 1967; Voll, 1967; Hartman *et al.*, 1971; Ely *et al.*, 1974). We developed a method for the selection of mutants with reduced expression of the first structural gene of the operon, *hisG* (Johnston & Roth, 1979). In addition to *hisG* mutants, the selection method yields mutants with defects in *hisO* that result in reduced operon expression. Because the target for mutation in this new selection scheme is only two genes, *hisO* mutants are more common (15% of total). We have used this selection method to isolate a large number of *hisO* mutants with reduced operon expression.

2. Materials and Methods

(a) *Properties of the histidine operon*

The histidine operon and biosynthetic pathway of *S. typhimurium* are diagrammed in Figure 1. The last step of the pathway is the conversion of histidinol to histidine, catalyzed by the product of the *hisD* gene. Histidine auxotrophs are able to grow with histidinol as a histidine source provided they express an intact *hisD* gene. Mutations in *hisD*, or mutations in the *his* control region that prevent operon (and hence *hisD*) expression, result in the inability to use histidinol as a histidine source (Hol$^-$ phenotype).

The *hisB* gene encodes the bifunctional enzyme that catalyzes the 7th and 9th steps of the biosynthetic pathway. One of the activities of this enzyme, the dehydratase reaction (7th

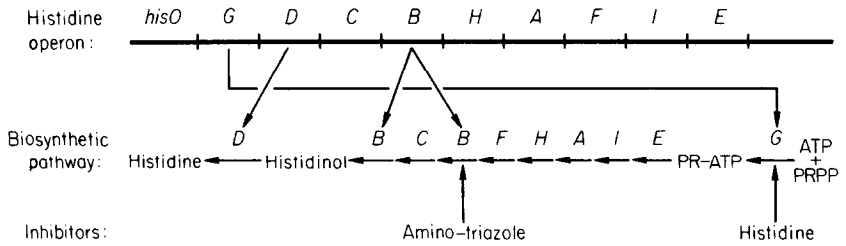

FIG. 1. The upper line represents the genes of the histidine operon. The middle part of the Figure is a diagram of the histidine biosynthetic pathway. The letters above the arrows correlate the genes with the enzymes of the pathway. The bottom line denotes the steps of the pathway that are inhibited by amino-triazole and histidine.

step), is inhibited by the drug amino-triazole (Hilton *et al.*, 1965). Wild-type cells challenged with amino-triazole become starved for histidine due to this inhibition, and respond by increasing *his* operon expression. The resultant increased *hisB* enzyme levels are sufficient to overcome the inhibition by amino-triazole. Therefore wild-type cells are resistant to the drug at a concentration of 40 mM. Mutants of the control region that are unable to increase operon expression in response to histidine starvation cannot grow in the presence of 40 mM-amino-triazole.

Constitutive mutants with high levels of operon expression, such as *hisT*$^-$ or *hisO*^{c}, have a wrinkled colony morphology on plates containing 2% (w/v) glucose (Roth *et al.*, 1966). This is a consequence of overproduction of the *hisF* and *hisH* enzymes (Murray & Hartman, 1972). Therefore, constitutive mutants that also possess a polar mutation in the *his* operon, or a mutation in the control region resulting in reduced expression of *hisH* and *hisF*, exhibit the normal smooth colony morphology (Fink *et al.*, 1967).

(b) *Selection method for mutants with reduced operon expression*

The method permits selection of mutants with reduced levels of *hisG* enzyme activity (Johnston & Roth, 1979). To summarize, it is based on the fact that the 1st step of the histidine biosynthetic pathway, catalyzed by the *hisG* enzyme, involves the consumption of ATP and PRPP. This reaction is normally closely regulated by feedback inhibition, and by repression of *hisG* synthesis. However, a mutant strain (TR5548) constitutive for operon expression (*hisT*$^-$) that also possesses a *hisG* enzyme resistant to feedback inhibition (*hisG*^{fr}), requires adenine, presumably due to the uncontrolled consumption of ATP in histidine biosynthesis. For unknown reasons, the adenine requirement occurs only at 42°C. Revertants (Ade$^+$) of TR5548 can be selected under these conditions. The majority of revertants carry mutations of the *hisG* gene, or mutations of the control region resulting in reduced operon expression.

(c) *Bacterial strains*

Multiply marked strains and their sources are listed in Table 1. All are derived from. *Salmonella typhimurium* strain LT2. All *his* auxotrophs were obtained from P. E. Hartman (Hartman *et al.*, 1971).

(d) *Media*

The composition of all media used here has been described (Johnston & Roth, 1979). Kanamycin sulfate was added at a final concentration of 50 μg/ml (rich medium), or 125 μg/ml (minimal medium).

TABLE 1

Multiply marked bacterial strains

Strain	Genotype	Source
TR3063	*hisO1242 hisΔOG8439*	Scott *et al.* (1975)
TR3064	*hisO1242 hisΔOG8440*	Scott *et al.* (1975)
TR3065	*hisO1242 hisΔOG8441*	Scott *et al.* (1975)
TR3066	*hisO1242 hisΔOG8442*	Scott *et al.* (1975)
TR3067	*hisΔOG8443*	Scott *et al.* (1975)
TR3068	*hisO1242 hisΔOG8444*	Scott *et al.* (1975)
TR3069	*hisO1242 hisΔOG8445*	Scott *et al.* (1975)
TR3070	*hisO1242 hisΔOG8446*	Scott *et al.* (1975)
TR3318	*hisO1242 hisΔOG8473*	Scott *et al.* (1975)
TR3319	*hisΔOG8472*	Scott *et al.* (1975)
TR3321	*hisΔOG8475*	Scott *et al.* (1975)
TR3456	*hisΔOG8495*	Scott *et al.* (1975)
TR3458	*hisΔOG8497*	Scott *et al.* (1975)
TR3473	*hisΔOG8512*	Scott *et al.* (1975)
TR3474	*hisΔOG8513*	Scott *et al.* (1975)
TR3475	*hisΔOG8514*	Scott *et al.* (1975)
TR3478	*hisΔOG8517*	Scott *et al.* (1975)
TR5107	*hisO1242 hisΔOG8664*	Johnston & Roth (1979)
TR5370	*hisΔOD9560*	Hoppe & Roth (unpublished results)
TR5380	*hisΔOD9570*	Hoppe & Roth (unpublished results)
TR5388	*hisΔD9578*	Hoppe & Roth (unpublished results)
TR5548	*hisG1102* (feedback resistant) *hisT1504*	Johnston & Roth (1979)
TR5549 thru TR5561	*hisO9607* thru *hisO9616 hisG1102 hisT1504*	See Table 3 for a complete description
TR5579 thru TR5632	*hisO9653* thru *hisO9706 hisG1102 hisT1504*	See Table 3 for a complete description
TR5717 thru TR5782	*hisO9709* thru *hisO9900 hisB1102 hisT1504*	See Table 4 for a complete description
TT1983	*hisO9529 zee-1*::Tn*10*	
TT2070	*supD* (sul) *zeb-618*::Tn*10 hisC527 leu-414*	J. Roth
TT2071	*supD*^{wt} *zeb-618*::Tn*10 hisC527 leu-414*	J. Roth
TT2158	*hisΔOD9552*	Hoppe & Roth (unpublished results)
TT2337	*supF* (su3) *zde-94*::Tn*10 hisC527 leu-414*	J. Roth
TT2342	*supE* (su2) *zbf-98*::Tn*10 hisC527 leu-414*	J. Roth
TT2345	*supC zde-605*::Tn*10 hisC527 leu-414*	J. Roth
TT3428	*hisΔ9708 hisT1504 pyrB64 metA53*	
TT3520	*hisO9609 hisG1102 hisT1504 recA1*	
TT3521	*hisO9653 hisG1102 hisT1504 recA1*	
TT3522	*hisO9654 hisG1102 hisT1504 recA1*	
TT3523	*hisO9663 hisG1102 hisT1504 recA1*	
TT3524	*hisO9675*	
TT3525	*hisO2321 hisG*$^{+}$ *hisT1504 recA1 zej-636*::Tn*5*	
TT3526	*hisΔOG203 hisT1504 recA1 zej-636*::Tn*5*	
TT3527	*hisG46 hisT1504 recA1*	
TT3528	*hisO9619 hisG1102 hisT1504 recA1*	
TT3529	*hisO9674 hisG1102 hisT1504 recA1 srl-211*::Tn*10*	
TT3530	*hisO9693 hisG1102 hisT1504 recA1 srl-211*::Tn*10*	
TT3531	*hisO9679 hisG1102 hisT1504 recA1 srl-211*::Tn*10*	
TT3532	*hisO9676 hisG1102 hisT1504 recA1 srl-211*::Tn*10*	
TT3533	*hisO9615 hisG1102 hisT1504 recA1 srl-211*::Tn*10*	
TT3534	*hisO9614 hisG1102 hisT1504 recA1 srl-211*::Tn*10*	

TABLE 1—*continued*

Strain	Genotype	Source
TT3535	*hisO9613 hisG1102 hisT1504 recA1 srl-211*::Tn*10*	
TT3536	*hisO9610 hisG1102 hisT1504 recA1 srl-211*::Tn*10*	
TT3537	*hisO9668 hisG1102 hisT1504 recA1 srl-211*::Tn*10*	
TT3539	*hisG1102 hisT1504 supE zde-94*::Tn*10*	
TT3540	*hisG1102 hisT1504 supC zde-605*::Tn*10*	
TT3541	*hisG1102 hisT1504 supD zeb-618*::Tn*10*	
TT3542	*hisO9663 hisG1102 hisT1504 supE zde-94*::Tn*10*	
TT3543	*hisO9663 hisG1102 hisT1504 supD zeb-618*::Tn*10*	
TT3544	*hisO9693 hisG1102 hisT1504 supE zde-94*::Tn*10*	
TT3546	*hisO9654 hisG1102 hisT1504 supC zde-605*::Tn*10*	
TT3574	*hisΔ9708 hisT1504 pyrB64 metA53*/F′600-1 *hisO-C→lacZ*	
TT3575	*hisΔ9708 hisT1504 pyrB64 metA53*/F′600-1 *hisO-C→lacZ hisG9648*::Tn*5*	
TT3590	*zee-4*::Tn*10 hisO3156 hisG46*	
TT3591	*zee-4*::Tn*10 hisO3199 hisG46*	
TT3592	*zee-4*::Tn*10 hisO1202 hisG46*	
TT3593	*zee-4*::Tn*10 hisO1812 hisG46*	
TT3594	*zee-4*::Tn*10 hisO3154 hisG46*	
TT3595	*zee-4*::Tn*10 hisO3197 hisG46*	
TT3597	*zee-4*::Tn*10 hisO3209 hisG46*	
TT3599	*zee-4*::Tn*10 hisO3216 hisG46*	
TT3600	*zee-4*::Tn*10 hisO3155 hisG46*	
TT4029	*hisO1242 hisB2135 supU1283 zhb-736*::Tn*10*	
TT5111	*hisD8468 aroD5 hisT1535* (ts) *strA1 recA1*/ F′600-5 *hisO-B→lacZ*	Chumley & Roth (1980)
TT5147	*hisD8468 aroD5 hisT1535* (ts) *strA1 recA1*/ F′600-1 *hisO-C→lacZ*	Chumley & Roth (1980)
TT5388	*zee-4*::Tn*10 hisO1832 hisG46*	
TT5390	*zee-4*::Tn*10 hisO3219 hisG46*	
TT5391	*hisO9676 hisG1102 zej-636*::Tn*5*	
TT5392	*hisO9679 hisG1102 zej-636*::Tn*5*	
TT5393	*hisO9689 hisG1102 zej-636*::Tn*5*	
TT5394	*hisO9685 hisG1102 zej-636*::Tn*5*	
TT5395 thru TT5411	*hisO*$^-$ *zee-4*::Tn*10 strA*^{wt}	
TT5412 thru TT5428	*hisO*$^-$ *zee-4*::Tn*10 strA1*	
TT5429	*hisΔ9708 hisT1504 pyrB64 metA53*/F′600-1 *hisO-C→lacZ hisD9639*::Tn*5*	
TT5430	*hisO9709 hisG1102 hisT1504 recA1 srl-211*::Tn*5*	
TT5431	*hisO9710 hisG1102 hisT1504 recA1 srl-211*::Tn*5*	
TT5432	*hisO9712 hisG1102 hisT1504 recA1 srl-211*::Tn*5*	
TT5433	*hisO9713 hisG1102 hisT1504 recA1 srl-211*::Tn*5*	
TT5434	*hisO9716 hisG1102 hisT1504 recA1 srl-211*::Tn*5*	
TT5435	*hisO9851 hisG1102 hisT1504 recA1 srl-211*::Tn*5*	
TT5436	*hisO9876 hisG1102 hisT1504 recA1 srl-211*::Tn*5*	

Unless otherwise noted, all strains were constructed for this study. The nomenclature of Tn*10* insertions is described by Chumley *et al.* (1979).

(e) *Transduction and mapping crosses*

The generalized transducing phage P22 (HT *int*$^-$) was used for all transductional and mapping crosses as previously described (Johnston & Roth, 1979; Hoppe *et al.*, 1979). Amino-triazole-sensitive *hisO* mutants, used as donors, were mapped with *hisO* deletion mutants, as recipients, selecting recombinants on minimal plates containing 40 mM-3-amino-

1,2-triazole, 0·5 mM-thiamine, 0·3 mM-L-methionine, and 0·005 mM-L-histidine. (This amount of histidine supports only very limited growth of the recipient strain, and is used only to increase the frequency of transduction.)

(f) *Reversion tests*

Reversion tests of His$^-$ *hisO* mutants were done as described by Johnston & Roth (1979). His$^+$ amino-triazole-sensitive mutants were tested for reversion by plating on minimal plates containing 40 mM-3-amino-1,2-triazole, 0·5 mM-adenine, 0·05 mM-thiamine and 0·005 mM-L-histidine, with a crystal of *N*-methyl-*N*-nitro-*N*-nitrosoguanidine, or a drop of 1 mg/ml solution of ICR191, or with no mutagen. Reversion frequencies are an average of at least 2 independent determinations.

(g) *Phenotypic suppression of* hisO *mutants by streptomycin*

Mutants to be tested were plated in soft agar on minimal plates containing 0·5 mM-adenine, 0·05 mM-thiamine, 0·3 mM-L-methionine and 0·005 mM-L-histidine. A few micrograms of streptomycin sulfate were placed in the middle of these plates. A ring of growth around the streptomycin after 3 days incubation at 37°C indicated that the mutation was suppressed by the drug.

(h) *Episome transfer*

The F′ episomes used for the dominance tests were transferred to F$^-$ recipients selecting for inheritance of the Tn*10* element (tetracycline resistance) present on the episomes. The counterselected mutations in the donor were either *pyrB64* and *metA53*, or *aroD5*. The donor and recipient were mated by cross-streaking on nutrient broth plates; cross-streaks were replica printed to selective medium to select exconjugants after overnight incubation.

(i) *Genetic nomenclature*

The *his* operon control region was originally designated *hisO*, by analogy to the *lac* operator locus, *lacO* (Roth *et al.*, 1966). However, it is becoming increasingly clear that the *his* operon is not controlled by a repressor protein, and thus possesses no true operator region. Nonetheless, in the desire to maintain continuity, we have chosen to continue calling the *his* control region *hisO*.

3. Results

(a) *Selection of* hisO *mutants*

The method used to isolate *hisO* mutants with reduced operon expression is a selection for mutants with reduced *hisG* expression (Johnston & Roth, 1979: summarized in Materials and Methods). The selection was carried out in the presence of histidine. This allows the recovery of mutants with no *hisG* expression (His$^-$) as well as those with only reduced *hisG* enzyme levels (His$^+$). Mutations in the control region can be distinguished from *hisG* mutations by their pleiotropic effect on the other genes of the *his* operon. Control region mutants completely unable to express the operon are His$^-$ and are also unable to grow on the biosynthetic intermediate histidinol (Hol$^-$ phenotype, see Materials and Methods). Mutants unable to derepress the operon are sensitive to the drug amino-triazole, which inhibits the *hisB* enzyme (see Materials and Methods). Furthermore, in the

presence of a *his* constitutive mutation (e.g. *hisT*), mutants with reduced operon expression exhibit a smooth colony morphology, whereas mutants with a normal *hisO* region have high levels of operon expression and have a rough colony morphology (see Materials and Methods). Therefore, in a *hisT*$^-$ background, we sought mutants having low *hisG* expression that formed smooth colonies. Such mutants were then scored for a Hol$^-$ or amino-triazole-sensitive (AT^S) phenotype. Many of these mutants proved to have defects mapping in the *hisO* region.

Mutants with reduced *hisG* expression were selected by plating strain TR5548 (*hisG1102 hisT1504*) on minimal plates containing histidine at 42°C. Under these conditions this strain requires adenine for growth; many of the revertants that no longer require adenine contain *his* mutations causing reduced *hisG* expression (Johnston & Roth, 1979; see Materials and Methods). Revertants (Ade$^+$) arise at a frequency of $7{\cdot}8 \times 10^{-5}$ per cell plated. Smooth colonies (2600 in 600 independent groups) were picked and tested for phenotype (Hol$^-$, AT^S). Mutants that are His$^+$ but sensitive to amino-triazole (about 13% of the total) were saved for further study. These are likely to contain mutations in *hisO* resulting in reduced operon expression. His$^-$ mutants whose histidine requirement is not satisfied by histidinol (about 20% of the total) can have mutations of two types: deletions of the structural genes that remove at least the *hisG* and *hisD* genes, or mutations in *hisO* that prevent operon expression. These two classes can be distinguished by genetic mapping of the His$^-$ mutations in question.

Two classes of mutants were immediately discarded. Mutants that are His$^-$ but Hol$^+$ (comprising about 50% of the total) are probably simple *hisG* mutants. Mutants that remain His$^+$ and resistant to amino-triazole (about 17%) are likely to contain mutations outside the *his* operon, in some other gene that serves to allow growth under the selection conditions. These two mutant classes were not studied further.

To identify the His$^-$Hol$^-$ mutants with *hisO* defects, the mutations in these strains were mapped by transduction. Generalized transducing phage P22 was grown on each of these His$^-$Hol$^-$ mutants (only one from any independent group, 446 in all) and used as a donor in crosses with His$^-$ point mutants as recipients. As expected, all of these mutants contain either deletions of at least the *hisG* and *hisD* genes, or mutations in *hisO*. Mutants containing mutations mapping entirely within *hisO* were picked for further study. This class included 65 mutants, or about 2% of the original mutants picked. All of the resulting *hisO* mutants are of independent origin.

(b) *Mapping of* hisO *mutations*

In the process of mapping these new His$^-$ *hisO* mutations, we discovered that many of them are deletions of various amounts of *hisO*. This allowed the construction of a fine structure deletion map of the control region. The His$^-$ *hisO* mutations were mapped by transduction selecting His$^+$ recombinants. The His$^+$ AT^S *hisO* mutants were used as donors in mapping crosses with His$^-$ *hisO* deletions as recipients; selection was made for His$^+$ amino-triazole-resistant recombinants. The map of *hisO* resulting from these crosses is presented in Figure 2. Under our

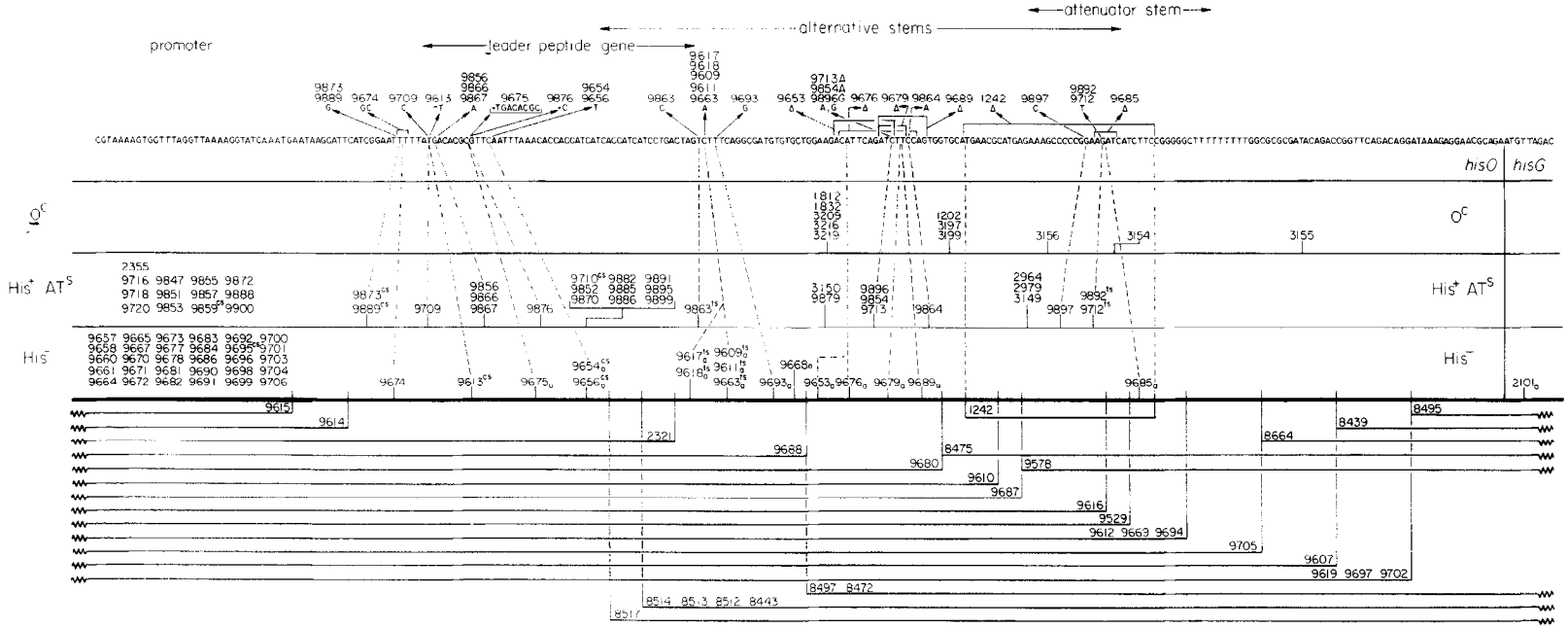

FIG. 2. Genetic and physical map of *hisO*. The bottom part of the Figure presents the genetic map of *hisO*. The broken lines correlate the mutations of the *hisO* DNA sequence in the upper part of the Figure. The mutations are gouped according to the phenotype they cause (see right- and left-hand columns). The point mutations that generate conditional phenotypes are designated: a, amber; o, ochre; u, UGA; cs, sold-sensitive; ts, heat-sensitive (see Tables 3 and 4). The wild-type DNA sequence was determined by Wayne Barnes, as was the sequence of mutations *hisO1242* and *hisO9656* (Barnes, 1978; personal communication). A number of other *hisOG* deletions map like *hisOG8439*. These include *hisOG8440*, *-8441*, *-8442*, *-8444*, *-8445*, *-8446*, *-8473*. The genetic mapping of three mutations does not agree with their placement on the DNA sequence. One case is *hisO9712* and *hisO9892*, which map between deletions 9687 and 9616. The other case is *hisO9876*, which maps between deletions 8514 and 8517. These discrepancies are probably due to the lower sensitivity of the crosses mapping the AT^S mutants (see Results, section (b)).

conditions, a cross between a wild-type donor and a His$^-$ *hisO* mutant yields about 10,000 His$^+$ recombinants per plate. A negative response represents no recombinants on at least five plates, or almost a 10^{-5}-fold reduction in recombination. The crosses on amino-triazole plates are about one-fourth as sensitive as this.

The deletions entering *hisO* from the *hisG* gene (from the right in Fig. 2) are *hisOG* deletions previously isolated using a different selection method (Scott *et al.*, 1975). All the *hisO* deletions isolated in this study enter the control region from the promoter–proximal side (from the left in Fig. 2). This is because only those *hisO* mutations that do not affect *hisG* were saved.

(c) *Mapping of* hisO *constitutive mutations*

A large number of mutants that have high levels of operon expression (*hisO*^{c}) have been isolated (Roth *et al.*, 1966; Chang *et al.*, 1971; Ely *et al.*, 1974). Although strains containing *hisO*^{c} mutations have no readily selectable phenotype, these mutations can be mapped because *hisO*^{c} mutants exhibit a wrinkled colony morphology. Wild-type (*hisO*$^+$) strains have a smooth colony morphology (see Materials and Methods). Therefore, the *hisO*^{c} mutations can be mapped in crosses with *hisO* deletion mutants by scoring the colony morphology of the recombinants. The strategy of these crosses is outlined in Figure 3. Each *hisO*^{c} mutation to be mapped is combined with a *hisG* mutation. This double mutant is used as recipient in crosses with *hisO* deletion mutants selecting for His$^+$ recombinants. If the *hisO* deletion does not cover the site of the *hisO*^{c} mutation, both rough and smooth recombinants are obtained; if the deletion covers the *hisO*^{c} site, only rough recombinants arise. Data for *hisO*^{c} mapping crosses are presented in Table 2, and the map positions of these mutations are shown in Figure 2.

(d) *Location of the hisO–hisG gene border on the genetic map*

The *hisO–hisG* gene border can be localized on the genetic map by two criteria. First, the ochre mutation *hisG2101* is the most *hisO*–proximal *hisG* mutation

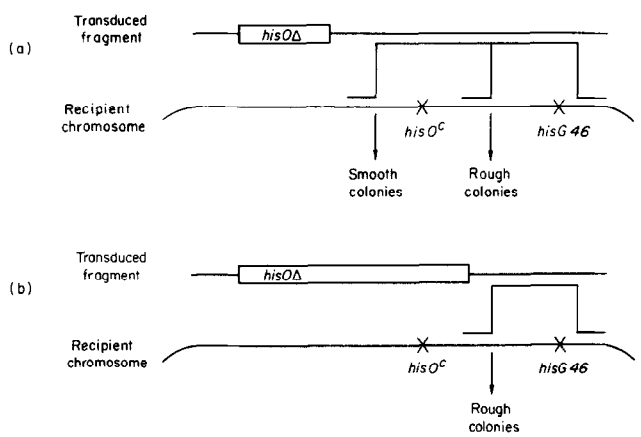

FIG. 3. Strategy of *hisO*^{c} mapping crosses. The rationale of the crosses is described in the text. In all cases the donor *hisO* deletions cause a His$^-$ phenotype.

TABLE 2

Results of hisO^c *mapping crosses*

		Recipient strain										
hisO^c Mutation	→	TT3599 3216	TT3597 3209	TT3593 1812	TT5388 1832	TT5390 3219	TT3595 3197	TT3592 1202	TT3591 3199	TT3590 3156	TT3494 3154	TT3600 3155	TR3063 1242
Donor													
hisO9614		52(268)		37(236)	31(147)	25(119)		46(188)	62(554)	33(118)	85(325)	84(210)	137(173)
hisO9688		10(437)	4(235)	3(275)	13(460)	25(622)	4(218)	16(422)	15(620)		154(1100)	128(496)	
hisO9680		0(503)	0(1788)	0(719)	0(223)	0(353)	1(1990)	1(1876)	1(1740)				4(766)
hisO9687		0(2454)	0(893)				0(1229)	0(3000)	0(1123)	4(2875)	5(2600)		0(776)
hisO9610		0(1026)	0(1500)	0(331)	0(231)		0(798)	0(3200)	0(3000)	7(463)	33(3150)	67(716)	0(1151)
hisO9616								0(3000)	0(2000)	0(2000)	6(2320)	16(460)	0(136)
hisO9529								0(1320)	0(1000)	0(1723)	0(2192)		0(104)
hisO9612				0(442)	0(405)			0(3000)	0(2000)	0(1100)	0(4400)	4(716)	0(14)
hisO9705												47(539)	
hisO9607												0(1298)	
hisO9619				0(724)					0(2500)	0(645)			

The crosses are diagrammed in Fig. 3. The recipient strains contained the *hisO*^{c} mutation and, in most cases, *hisG46* (TR3063 contained *hisO*^{c}*1242*] and *hisOG8439*). Phage P22 grown on the donor strains (TR5614, TR5606, TR5552, TR5613, TT1983, TR5558, TR5554, TR5631, TR5549) infected the recipients, and the resulting His$^+$ recombinants were scored for rough or smooth colony morphology. Reported are the number of smooth recombinants and the total number of His$^+$ recombinants scored (in parentheses).

(Hoppe *et al.*, 1979). Thus, the gene border must lie to the left of this mutation. Second, two of the longest *hisO* deletions, *hisO9607* and *hisO9619*, revert to His^+ at low frequency (10^{-10}). It is highly unlikely this could occur if these deletions entered *hisG*. Therefore, the *hisO–hisG* gene border most likely lies between *hisO9619* and *his2101*.

(e) *Correlation of physical and genetic* hisO *maps*

In the accompanying paper (Johnston & Roth, 1980) we describe the DNA sequence alterations of many of the *hisO* mutations. These results are presented here, in Figure 2, to correlate the genetic map with the DNA sequence of the *his* control region. All constitutive mutations (*hisO*^{c}) presented here map in or near the attenuator (defined by mutation *hisO1242*, which deletes two-thirds of attenuator stem sequences). These constitutive mutations probably affect the stability or formation of the attenuator stem. The region between the deletion endpoints of *hisO9614* and *hisO2321* includes *his* leader peptide gene and its ribosome binding site. The two deletion intervals between the endpoints of *hisO2321* and *hisOG8475* include the region of alternative mRNA stem-loop structures between the leader peptide gene and the attenuator stem. The region removed by the *hisO9615* deletion probably includes the *his* promotor (see Discussion).

(f) *Phenotype of* hisO *mutants*

The mutants of the *his* control region obtained in this study are of two phenotypic classes: (1) His^- mutants (completely unable to express the operon); and (2) His^+ mutants that express the operon at a low level, but are unable to achieve fully derepressed levels of operon expression in response to histidine starvation (sensitive to amino-triazole). The mutations resulting in these phenotypes are identified on the *hisO* genetic map (Fig. 2), and are listed in Tables 3 and 4. Both deletion and point mutations are among the His^- class; only point mutations are among the amino-triazole-sensitive mutants.

In the process of characterizing these mutants we discovered that some of them show a temperature-dependent His phenotype: some *hisO* mutants are heat-sensitive, and some are cold-sensitive. These data are summarized in Tables 3 and 4, and the mutations causing these phenotypes are identified in Figure 2. The basis of the temperature effect on these mutants is discussed more fully in the accompanying paper (Johnston & Roth, 1980).

(g) *Reversion of* hisO *mutants*

(i) *Reversion of* His^- hisO *mutants*

To further characterize the *hisO* mutants, we tested their ability to revert, both spontaneously and when induced by mutagens. The result of these tests for the His^- *hisO* mutants are summarized in the last two columns of Table 3. Most of the *hisO* deletions revert to His^+ at a low frequency spontaneously, and are not

TABLE 3

Properties of His⁻ hisO *mutants*

Strain	*hisO* mutation	Spontaneous reversion		Induced reversion
Deletion mutations				
TT1983	9529	+	6×10^{-8}	NG
TR5549	9607	−		
TR5552	9610	−		
TR5554	9612	±		
TR5556	9614	±		
TR5557	9615	−	$<10^{-8}$	
TR5558	9616	−		
TR5561	9619	−		
TR5595	9669	±		NG
TR5606	9680	+	6×10^{-8}	NG, ICR
TR5613	9687	−		
TR5614	9688	±	2×10^{-8}	NG
TR5620	9694	±		NG
TR5623	9697	−		
TR5628	9702	±		
TR5631	9705	−		
Promotor mutations				
TR5583	9657	−	3×10^{-9}	NG
TR5584	9658	±		NG
TR5586	9660	−		NG
TR5687	9661	+	3×10^{-8}	NG
TR5590	9664	−		NG
TR5591	9665	−		NG
TR5593	9667	−	1×10^{-9}	NG
TR5596	9670	+		NG
TR5597	9671	+		NG
TR5598	9672	−		NG
TR5599	9673	−		
TR5603	9677	+		NG, ICR
TR5604	9678	−	$<10^{-9}$	NG
TR5607	9681	+		NG
TR5608	9582	+		NG
TR5609	9683	+		NG, ICR
Promotor mutations				
TR5610	9684	+		NG, ICR
TR5612	9686	±		NG
TR5616	9690	−		NG
TR5617	9691	+		NG
TR5618	9692	±		NG
TR5621	9695cs	+		NG
TR5622	9696	±		
TR5624	9698	+		NG
TR5625	9699	±		NG
TR5626	9700	±		NG
TR5627	9701	±		NG
TR5629	9703	+		NG
TR5630	9704	±		NG
TR5632	9706	±		NG
Leader peptide gene and stem mutants				
TR5551	9609ts,a	++	4×10^{-7}	NG, ICR
TR5553	9611ts,a	++		NG, ICR
TR5554	9613	++	5×10^{-7}	NG, ICR
TR5559	9617ts,a	++		NG, ICR
TR5560	9618ts,a	++		NG, ICR
TR5579	9653ts,a	++	2×10^{-5}	NG, ICR
TR5580	9654cs,o	++	2×10^{-6}	NG, ICR
TR5582	9656cs,o	++		NG, ICR
TR5589	9663ts,a	++	3×10^{-7}	NG, ICR
TR5594	9668a	++		NG, ICR
TR5600	9674	++	7×10^{-8}	NG, ICR
TR5601	9675cs,u	++	1×10^{-6}	NG, ICR
TR5602	9676ts,a	++		NG, ICR
TR5605	9679a	++	1×10^{-7}	NG, ICR
TR5611	9685L	++	1×10^{-6}	NG, ICR
TR5615	9689a	++		NG, ICR
TR5619	9693a	++	1×10^{-7}	NG, ICR

Properties of His^- *hisO* mutants and His^+ AT^S *hisO* mutants. cs: mutant is His^- (or AT^S) at 30°C, His^+ (or AT^R) at 42°C: ts: mutant is His^- (or AT^S) at 42°C, His^+ (or AT^R) at 30°C: a, amber: o, ochre: u, UGA: mutation is suppressed by these types of supressors: L, mutant is weakly His^+ (i.e. leaky). Qualitative spontaneous reversion frequencies represent the number of His^+ (or AT^R) revertants per 2×10^8 cells plated: −, 0 His^+ revertants: + −, 1 to 10 His^+ revertants: +, 10 to 100 His^+ revertants: ++ >100 His^+ revertants. The mutagens *N*-methyl-*N*-nitro-*N*-nitrosoguanidine (NG) and ICR191 and ICR3640H were tested for the ability to induce reversion as described in Materials and Methods.

induced to revert by mutagens. Some deletions are induced to revert to His^+ by nitrosoguanidine, which causes base substitution mutations. The revertant lesions probably create a new promoter, or serve to fuse the *his* operon to a pre-existing "foreign" promoter. The His^- point mutations at the far left of the map (i.e. mapping under deletion *hisO9615*) all revert to His^+ at a low frequency: some are

TABLE 4

Properties of His$^+$ amino-triazole-sensitive hisO *mutants*

Strain	*hisO* mutation	Spontaneous reversion	Induced reversion	Strain	*hisO* mutation	Spontaneous reversion	Induced reversion
TR5715	9709	±	NG	TR5749	9867	±	
TR5718	9710cs	±	NG	TR5752	9870	±	
TR5720	9712ts	−	NG	TR5754	9872	−	
TR5721	9713	±	NG	TR5755	9873cs	−	NG
TR5724	9716	−	NG	TR5758	9876	+	
TR5726	9718	±		TR5761	9879	−	
TR5728	9720	±	NG	TR5764	9882	±	
TR5729	9847	−		TR5767	9885	±	
TR5733	9851	−	NG	TR5768	9886	±	
TR5734	9852	±		TR5770	9888	−	NG
TR5735	9853	±	NG	TR5771	9889cs	±	NG
TR5736	9854	±	NG	TR5773	9891	−	NG
TR5737	9855	±		TR5774	9892ts	−	NG
TR5738	9856	±		TR5777	9895	±	
TR5739	9857	±		TR5778	9896	±	NG
TR5741	9859cs	±	NG	TR5779	9897	±	NG
TR5745	9863ts	−	NG	TR5781	9899	±	
TR5746	9856	±	NG	TR5782	9900	−	
TR5748	9866	−	NG				

Properties of His$^-$ *hisO* mutants and His$^+$ AT^S *hisO* mutants. cs: mutant is His$^-$ (or AT^S) at 30°C, His$^+$ (or AT^R) at 42°C; ts: mutant is His$^-$ (or AT^S) at 42°C, His$^+$ (or AT^R) at 30°C; a, amber; o, ochre; u, UGA: mutation is suppressed by these types of supressors: L, mutant is weakly His$^+$ (i.e. leaky). Qualitative spontaneous reversion frequencies represent the number of His$^+$ (or AT^R) revertants per 2×10^8 cells plated: −, 0 His$^+$ revertants; + −, 1 to 10 His$^+$ revertants; +, 10 to 100 His$^+$ revertants; ++ >100 His$^+$ revertants. The mutagens *N*-methyl-*N*-nitro-*N*-nitrosoguanidine (NG) and ICR191 and ICR3640H were tested for the ability to induce reversion as described in Materials and Methods.

induced to revert only by nitrosoguanidine, others by nitrosoguanidine and ICR191. Many of these mutations are likely to affect the *his* promoter (see Discussion).

The His$^-$ point mutations mapping in the middle of the control region (i.e. the 16 His$^-$ mutations mapping between *hisO9615* and *hisOG8475*) all revert to His$^+$ at a very high frequency spontaneously, and are induced to revert by both nitrosoguandine and ICR191. The high spontaneous reversion frequency of these mutations, and the fact that their reversion is induced by both base-substitution and frameshift-inducing mutagens strongly suggests that their reversion is not due to correction of the original mutation. Instead, it is likely that these revertants contain second-site mutations in the *his* control region that suppress the *hisO* mutations (see below).

(ii) *Many His$^+$ revertants are due to second site suppressors*

Strains containing the *hisT* mutation and a wild-type *his* operon exhibit a wrinkled colony morphology due to derepression of the *his* operon caused by the *hisT* mutation. Mutations that reduce operon expression cause a smooth colony morphology in *hisT* mutants (see Materials and Methods). Since the reversion of the

hisO mutations was done in *hisT*$^-$ strains, His$^+$ revertants due to back mutation of the *hisO* lesion would have the wrinkled colony morphology characteristic of *hisT* mutants. However, all of the His$^+$ revertants of the 16 unstable *hisO* mutants form smooth (*hisO*$^+$) colonies. Therefore, a second mutation must cause the His$^+$ phenotype, but provide only a low level of operon expression. The second-site mutations in eight of the His$^+$ revertants (3 His$^+$ revertants of *hisO9675*, 3 revertants of *hisO9654*, and 2 revertants of *hisO9663*) have been mapped and found to lie within the *his* control region; all lie under deletion *hisOG203*, which deletes the control region and the first half of the *hisG* gene (data not shown).

The current model for operon regulation (Johnston *et al.*, 1980) suggests an explanation for the instability of the *hisO* mutations mapping between the attenuator and promotor. These mutations all affect *his* leader mRNA secondary structure and are His$^-$ presumably due to excessive attenuator stem formation (Johnston *et al.*, 1980: see accompanying paper, Chumley & Roth, 1980). Any mutation that reduces the stability or prevents formation of the attenuator stem should suppress these His$^-$ regulatory mutations. The large number of ways of doing this would explain the high reversion frequency of these mutations.

(iii) *Reversion of His$^+$ AT^S mutants*

Most of the amino-triazole-sensitive mutants revert to resistance to this drug, but at a frequency much lower than for reversion of the His$^-$ mutants to His$^+$ (Table 4). This is expected, since resistance to 40 mM-amino-triazole requires a high level of operon expression (at least 5 × basal level), while only a very low level of operon expression (about 0·1 basal level) is required for a His$^+$ phenotype. Therefore, a more limited set of mutations, those drastically reducing attenuator function, would be expected to suppress the AT^S defects.

(h) *Informational suppression of* hisO *mutations*

Translation of the *hisO* region is required for *in vitro* transcription of the *his* operon to proceed through the attenuator and into the structural genes (Artz & Broach, 1975). We reasoned that if any of the His$^-$ *hisO* mutations blocked translation by generating a nonsense codon in the translated region of *hisO*, they might be suppressed by nonsense suppressors. To test this possibility, we transduced each His$^-$ *hisO* mutation into recipients carrying a large *his* deletion and one of several nonsense suppressors. A large number of prototrophic recombinants (His$^+$) arising from these crosses indicate that the donor *hisO* mutation is suppressible. As a result of this test, we identified a number of *hisO* mutations suppressible by nonsense suppressors. All three nonsense types are represented, including 11 amber (UAG) mutations (*hisO9619*, *-9611*, *-9617*, *-9618*, *-9653*, *-9663*, *-9668*, *-9676*, *-9679*, *-9689*, *-9693*): two ochre (UAA) mutations (*hisO9654*, *-9656*) and one UGA mutation (*hisO9675*). These mutations are identified on the genetic map (Fig. 2). The amber-suppressible mutations in *hisO* do not generate UAG codons; these mutations are discussed in detail in the accompanying paper (Johnston & Roth, 1980).

To confirm these results and determine the pattern of suppression for each of these mutations, several well characterized nonsense suppressor mutations (Winston *et al.*, 1979) were transduced into the *hisO* nonsense mutants. Strains carrying various nonsense suppressor mutations linked to a Tn*10* insertion were constructed by a recently described technique (Kleckner *et al.*, 1977). Phage P22 grown on these strains was used to transduce the Tn*10* insertions into *hisO* nonsense mutants, selecting tetracycline-resistant recombinants. Co-inheritance of the linked suppressor mutation results in a His^+ phenotype if the *hisO* mutation is suppressed; if the suppressor is unable to supress the *hisO* mutation, all of the tetracycline-resistant recombinants remain His^-.

The results of these crosses are presented in Table 5. All the *hisO* amber mutations are suppressed by the tyrosine-inserting amber suppressor *supF* and by the serine-inserting *supD* amber suppressor. Some are suppressed by the *supC* ochre suppressor. None is suppressed by *supE*, probably due to the presence of a $hisT^-$ mutation in these strains, which is known to drastically reduce the suppression efficiency of *supE* (Bossi & Roth, 1980). The two *hisO* ochre mutations are suppressed only by the *supC* ochre suppressor. The *hisO* UGA mutation is

TABLE 5

Suppression of hisO *nonsense mutations*

Recipient strain	*hisO* mutation	Suppressor tested: None *supD*^{wt}	Amber *supD*	Amber *supE*	Amber *supF*	Ochre *supC*	UGA *supU*	Mutation type
TR5551	*hisO9609*	—	±33	—	+55	—		Amber
TR5579	*hisO9653*	—	±50	—	+50	±48		Amber
TR5589	*hisO9663*	—	±47	—	+42	±45		Amber
TR5594	*hisO9668*	—	±38	—	+45	±45		Amber
TR5602	*hisO9676*†	—	±46		±40	±26		Amber†
TR5605	*hisO9679*†	—	±48		±22	—		Amber†
TT5394	*hisO9685*‡	—	±40		± 6	—		Amber‡
TR5615	*hisO9689*†	—	±52		±20	—		Amber†
TR5619	*hisO9693*	—	±23	—	+50	—		Amber
	hisB527	—	+50	+68	+68	+51		Amber
TR5580	*hisO9654*	—	—	—	—	+48		Ochre
TR5582	*hisO9656*	—	—	—	—	+55		Ochre
	hisC117	—	—	—	—	+41		Ochre
TR5601	*hisO9675*						+6	UGA
	hisB2135						+9	UGA

Transducing phage P22 grown on the donor strains (TT2070, TT2071, TT2337, TT2342, TT2345 and TT4029) transduced the recipient *hisO* mutants to tetracycline resistance. The Tet^R recombinants were replica printed to test their His phenotype. A (+) signifies that some of the Tet^R recombinants were also His^+, and must therefore have inherited the suppressor mutation linked to the Tn*10* element. A (±) signifies that the strain grows poorly without histidine: the suppressor only partially corrects the mutational defect. The percentage His^+ recombinants is in parentheses (approximately 50 to 100 Tet^R recombinants scored). A (−) signifies that none of the Tet^R recombinants was His^+. All recipients, except *hisB527*, *hisC117*, *hisB2135* and TT5394, carry the *hisT1504* and *hisG1102* (feedback resistance) mutations.

† These mutations are especially weakly suppressed in $hisT^-$ strains; suppression is markedly stronger in $hisT^+$ strains.

‡ This mutation is not suppressed in $hisT^-$ strains, and is only weakly suppressed in $hisT^+$ strains.

suppressed by *supU*, a recently isolated UGA suppressor mapping near *strA* (*rpsL*) (Johnston & Roth, unpublished results).

To quantitate the level of suppression, we assayed *hisB* enzyme (histidinol phosphate phosphatase) levels in strains containing *hisO* mutations with and without the appropriate suppressors (Table 6). Enzyme levels in *hisO* mutants carrying a nonsense supressor are substantially increased compared to the strains with no suppressor.

TABLE 6

hisB *enzyme levels in suppressed* hisO *nonsense mutants*

Strain	*hisO* mutation	Type	Suppressor present	*hisB* enzyme specific activity
TR5589	*hisO9663*	Amber	None	<0·13
TT3542	*hisO9663*	Amber	*supF* amber	0·54
TT3543	*hisO9663*	Amber	*supD* amber	0·15
TR5619	*hisO9693*	Amber	None	<0·13
TT3544	*hisO9693*	Amber	*supF* amber	0·35
TR5580	*hisO9654*	Ochre	None	0·23
TT3546	*hisO9654*	Ochre	*supC* ochre	1·11
TR5548	*hisO*$^+$ (*hisT*$^-$)		None	21·1
LT2	*hisO*$^+$ (*hisT*$^+$)		None	1·76

Histidinol phosphate phosphatase (*hisB*) enzyme levels in *hisO* nonsense mutants. Strains grown at 37°C in minimal medium containing 0·1 mM-L-histidine were assayed as described by Martin *et al.* (1971). Enzyme levels due to *hisB* expression from the internal *his* promotor between *hisG* and *hisB* (P2, spec. act. 0·61) have been subtracted from all values. All strains are isogenic. All strains, except LT2, carry the *hisT1504* and *hisG1102* (feedback resistance) mutations.

All the *hisO* mutations suppressible by nonsense suppressors map in the central region of the genetic map, between the promotor (*hisO9615*) and the attenuator (*hisO1242*) (Fig. 2). These mutations demonstrate that a region of *hisO* between the promotor and the attenuator is translated into protein. The DNA sequence changes of these mutations have been determined (Johnston & Roth, 1980); they all affect either the translation of the *his* leader peptide gene or the stability of *his* leader mRNA secondary structure.

(i) *Correction of nonsense* hisO *mutations by streptomycin*

The drug streptomycin induces misreading of the genetic code by the translation apparatus. Sub-lethal levels of streptomycin suppress many nonsense mutations by causing polypeptide chain termination codons to be read as sense (amino acid) codons at a low level. This phenotypic correction does not occur in *strA* mutant strains due to an alteration of one of the proteins of the small ribosomal subunit that reduces the level of misreading (Gorini, 1971).

To confirm that suppression of the *hisO* mutations by nonsense suppressors is occurring at the level of translation, we tested the ability of the drug streptomycin

to phenotypically correct several His$^-$ *hisO* mutations. Table 7 shows that the nonsense-suppressible *hisO* mutations are corrected by low levels of streptomycin, but only in a *strA*^{wt} genetic background, not in a *strA*^{R} background. This is strong evidence that a region of *hisO* is translated into protein.

TABLE 7

Phenotypic suppression of hisO *mutations by streptomycin*

Mutation	Type	Correction by streptomycin in strains containing these *strA* alleles	
		strA^{wt}	*strA1*
hisO9609	Amber	+	−
hisO9613	Deletion	−	−
hisO9653	Amber	+	−
hisO9654	Ochre	+	−
hisO9656	Ochre	+	−
hisO9663	Amber	±	−
hisO9668	Amber	+	−
hisO9674	Point	±	−
hisO9675	UGA	+	−
hisO9676	Amber	+	−
hisO9679	Amber	+	−
hisO9693	Amber	±	−
hisO2321	Deletion	−	−
hisG205	UGA	+	−
hisC527	Amber	+	−
hisC117	Ochre	±	−
hisG8655	Frameshift	−	−

Suppression was tested as described in Materials and Methods. The strength of suppression was scored qualitatively. Each mutation was tested in both a *strA*^{WT} and a *strA*^{R} genetic background. All strains are isogenic (TT5395 to TT5428, see Table 1).

(j) *Dominance tests of* hisO *mutations*

(i) *Dominance of His*$^-$ hisO *mutations*

The existence of nonsense and temperature-sensitive mutations in the *his* control region suggested the presence of a gene involved in operon regulation. Determination of the DNA sequence changes of the nonsense *hisO* mutations revealed that this gene is the *his* leader peptide gene, which codes for a polypeptide of 16 amino acids containing seven histidine residues in tandem (Barnes, 1978: DiNocera *et al.*, 1978; Johnston *et al.*, 1980). To determine if this gene encodes a diffusible product, we tested the dominance of a number of *hisO* mutations.

The diploid strains used for the dominance tests carry a wild-type *hisO* region on an F′ episome, and a mutant *hisO* region in the chromosome. The episomes used for these tests were specially constructed F′128 plasmids that contain the *Salmonella his* control region and the first two (or three) *his* structural genes fused to the *E. coli lacZ* gene (Chumley & Roth, 1980). The structure of these episomes and the strategy of the dominance tests are outlined in Figure 4.

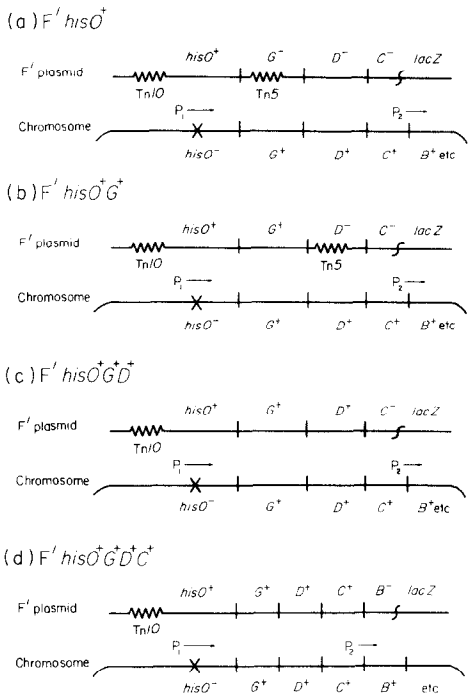

FIG. 4. Diagram of diploid strains used in dominance tests of *hisO* mutations. The chromosome in each case contains one of the *hisO* mutations listed in Table 7. P1 is the primary, regulated *his* operon promotor that lies in *hisO*. P2 is the secondary, unregulated promotor that lies between *hisC* and *hisB* (Ely & Ciesla, 1974), and causes constitutive, low level expression of all *his* genes downstream of *hisC*. The episomes used carry the first few genes of the *his* operon fused to *lacZ* (Chumley & Roth, 1980); their structure is detailed in Results, section (j). The plasmids all carry a Tn*10* insertion near, but not in, the *hisO* gene (*zee-4*::Tn*10*); this Tn*10* element was used to select for transfer and maintainance of the plasmid. The full genotypes of these plasmids are presented in Table 1 (strains TT3574, TT3575, TT5111, TT5147 and TT5429).

In each case, the *hisO* mutation to be tested is in the chromosome, *cis* to intact structural genes. Growth of the *hisO* mutants is limited only by their reduced expression of the first three structural genes, *hisG*, *hisD* and *hisC*; the other structural genes are expressed, at levels sufficient to yield a His^+ phenotype, from the unregulated internal *his* promoter P2, located between the *hisC* and *hisB* genes (Ely & Ciesla, 1974; Kleckner *et al.*, 1977; M. Schmid, unpublished results). Four different F′ *his–lac* fusion episomes were used, each carrying different amounts of an intact *his* operon. The episome diagrammed in Figure 4(a) carries only an intact *hisO* gene; all the *his* genes downstream of *hisD* are deleted due to the *hisC–lacZ* fusion on this plasmid; the *hisG* and *hisD* genes are inactivated by a Tn*5* insertion in *hisG*. The episome in Figure 4(b) is the same as that in Figure 4(a), except that the *hisG* gene is functional, while *hisD* is inactivated by a Tn*5* insertion ($hisO^+G^+$). Figure 4(c) shows the same episome without the Tn*5* insertion; therefore this episome carries $hisO^+G^+D^+$. The episome in Figure 4(d) contains a *his* operon fused to *lacZ* in the *hisB* gene. This plasmid is functional for the *hisO* region and all of the first three *his* structural genes ($hisO^+G^+D^+C^+$).

Diploid strains of the types diagrammed in Figure 4 were constructed and their *his* phenotype scored. These results are presented in Table 8: a minus in the Table denotes that the diploid strain is His^-; a plus means the strain is His^+. Dominance tests of *hisO* point mutations are presented in the upper half of Table 8; the lower half of the Table presents dominance tests of deletions of the control region, all of which presumably remove the *his* promotor. Column 2 presents the phenotype of strains of the type diagrammed in Figure 4(a). The only functional *hisO* region in these strains is on the plasmid, and is unable to provide (in *trans*) the function missing from the mutant chromosomal *hisO* region. Therefore, the *hisO* mutations are dominant.

Column 5 in Table 8 shows that all strains of the type diagrammed in Figure 4(d) are His^+. This means that the *hisG*, *hisD* and *hisC* genes on the plasmid are expressed in these strains. Therefore, the chromosomal *hisO* mutations impair the function of only those genes located *cis* to the *hisO* mutation. Thus, columns 2 and 5 demonstrate that all of the *hisO* mutations tested are *cis*-dominant. From these results, we conclude that the leader peptide gene product either has no function, or is a *cis*-acting protein.

The phenotypes of strains of the type diagrammed in Figure 4(c) are presented in

TABLE 8

Dominance tests of hisO *mutations*

Chromosomal mutation	His phenotype of diploid strains containing these episomes: F'*hisO*$^+$	F'*hisO*$^+$*G*$^+$	F'*hisO*$^+$*G*$^+$*D*$^+$	F'*hisO*$^+$*G*$^+$*D*$^+$*C*$^+$	F'
hisO9653	−	+	+(215)	+	−(>600)
hisO9654	−	+	+(100)	+	±(430)
hisO9676	−	+	+	+	−
hisO9679	−	+	+	+	−
gisO9663	−	±	+(260)	+	−(>600)
hisO9609	−	±	+(215)	+	−(>600)
hisO9693	−	±	+	+	−
hisO9613	−	−	+	+	−
hisO9668	−	−	+	+	−
hisO9674	−	−	+	+	−
hisO9675	−	−	+(240)	+	−(>600)
hisO9610	−	−	−	+	−
hisO9614	−	−	−	+	−
hisO9615	−	−	−	+	−
hisO9619	−	−	−	+	−(>600)
hisO2321	−	−	−(>510)	+	−(>600)
hisOG203	−	−	−	+	−
hisG46	−	+	+(60)	+	−(>600)

Diploid strains of the type diagrammed in Fig. 4 were constructed and tested for their His phenotype. The plasmids (in strains TT3574, TT3575, TT5111, TT5147 and TT5429) were transferred to recipient *hisO* mutants and maintained by selecting for the Tn*10* insertion present in the plasmid. The diploid strains were then tested for the ability to grow on minimal medium (His^+). A (+) indicates the diploid strain is His^+; A (−) signifies the diploid strain is His^-. The numbers in parentheses are doubling times in minutes of the diploid strains growing in minimal medium at 37°C. All recipient strains (TT3520 to TT3537, see Table 1) contain *recA1*, *hisT1504*, *hisG1102* (feedback resistant), except *hisO2321*, *hisOG203* and *hisG46*, which contain *recA1* only.

Table 8 column 4. These strains carry functional *hisO*, *hisG* and *hisD* genes on the episome, but the only functional *hisC* gene is in the chromosome, *cis* to the *hisO* mutation. Diploid strains containing a *hisO* deletion mutation are His^- because they are unable to express the chromosomal *hisC* gene (bottom half of Table 8, column 5). However, in diploids containing a *hisO* point mutation, the *hisC* gene *cis* to the *hisO* mutation must be expressed, since these strains are His^+ (top half of Table 8, column 5). The *hisC* gene must be expressed at a low level, however, because the growth rates of these strains are considerably slower than for a diploid strain carrying a chromosomal *hisG* mutation, which contains a full complement of *his* enzymes (line 18, column 4). The phenotypes of the diploid strains presented in column 3 suggest that some of the *hisO* point mutants require only the *hisG* gene product to be His^+. The episome in these strains carries a $hisO^+$ and a $hisG^+$ gene, but the only intact *hisD* and *hisC* genes are in the chromosome, *cis* to the *hisO* mutation. Nevertheless, some of these diploids are His^+ (e.g. *hisO9654*), and must therefore express the chromosomal *hisD* and *hisC* genes at some low level.

Therefore, some of the *hisO* point mutants require both *hisG* and *hisD* gene products for a His^+ phenotype, while some of the other *hisO* mutants require only the *hisG* gene product. This probably reflects different residual levels of expression in the two classes of mutants. The *hisO* deletion mutants tested, which probably remove the promotor, must have no residual operon expression, since they are unable to provide *hisG*, *hisD*, or *hisC* function (see bottom half of Table 8, column 4).

(ii) *Dominance of* His^+ hisO *mutations*

The His^+ AT^S *hisO* mutations were also tested for dominance. These mutants are sensitive to the drug amino-triazole, which inhibits one of the reactions catalyzed by the *hisB* enzyme. Wild type is resistant to amino-triazole because it increases operon expression (and hence *hisB* enzyme levels) when challenged with the drug (see Materials and Methods).

The strategy of these complementation tests is similar to that for the His^- *hisO* mutants. The episome diagrammed in Figure 4(a) was introduced into the His^+ *hisO* mutants. If the $hisO^+$ gene on the plasmid can provide in *trans* the function missing from the chromosomal *hisO* region, then the diploid strain will be able to increase operon expression when challenged with amino-triazole, and will therefore be resistant to the drug. If the *hisO* mutation is dominant, the diploid will be sensitive to amino-triazole. All of the mutants tested (*hisO9709*, *–9710*, *–9712*, *–9713*, *–9716*, *–9851*, *–9876*) remained sensitive to amino-triazole when made diploid for *hisO* with the episome diagrammed in Figure 4(a). This demonstrates that the His^+ *hisO* mutants are also dominant.

4. Discussion

We have isolated and characterized a large number of histidine operon regulatory mutants with defects of the *his* control region. The determination of the DNA sequence changes of a number of these mutations, presented in the

accompanying paper, has allowed a correlation of the *hisO* genetic map with the DNA sequence. Consequently, the regions of the genetic map representing the attenuator, the leader peptide gene, and the region of alternative mRNA stem-loop structures located between these two sites have been precisely identified (Fig. 2).

Three pieces of evidence suggest that many of the mutations that map under deletion *hisO9615* (at the far left in Fig. 2) probably affect the *his* promotor. First, the deletions that enter *hisO* from *hisG* all have a right endpoint within *hisG* and still express the intact *hisD* gene. The deletion of this type that removes the largest part of *hisO* is *hisOG8517*, and therefore the *his* promoter must lie to the left of this deletion. Second, the deletion *hisO9615* is the leftmost His^- deletion and, since it does not enter the *his* leader peptide gene (see Fig. 2), its His^- phenotype is most likely due to removal of the promotor. Finally, the *hisO2355* mutation has the phenotype expected of a promotor mutation (Ippen *et al.*, 1968): it has low levels of operon expression, but can be derepressed over the same 20-fold range as wild type (Ely, 1974).

All of the *hisO* mutations tested here, as well as those tested previously, are *cis*-dominant (Fink & Roth, 1968; Ely, 1974). This result is expected for promotor and attenuator mutations. Since mutations altering the *his* leader peptide gene (e.g. *hisO9709*, *-9876*, *-9654*, and *hisO9675*) are not complemented in *trans* by a wild-type *hisO* region, the product of this gene must either have no function, or it must be a *cis*-acting protein. These two possibilities are discussed in the accompanying paper (Johnston & Roth, 1980).

The results of the dominance tests (Table 8) reveal that the His^- point mutants all have a very low level of residual operon expression. Some of these mutants are His^- because their growth is limited only by their low level of *hisG* gene product (e.g. *hisO9654*); the rest require both the *hisG* and *hisD* enzymes (e.g. *hisO9675*). The fact that *hisG* enzyme becomes limiting first as operon expression is reduced is not surprising. Since this enzyme catalyzes the feedback inhibitable first step of the biosynthetic pathway, it might be expected to be the rate-limiting reaction. Since none of the point mutants requires a functional *hisC* gene on the plasmid for a His^+ phenotype (Table 4, column D), all must express their chromosomal *hisC* gene at some level. Apparently, none of the point mutations causes an absolute block in readthrough of the attenuator site.

The *hisO* genetic map presented in Figure 2 is an extension and revision of an earlier map based on three-point transductional crosses (Ely *et al.*, 1974). In most respects, our map agrees with that produced earlier. Both show groups of mutations causing high levels of operon expression interspersed among groups of mutations causing reduced operon expression. This map distribution fits well with the model for histidine operon regulation (Johnston *et al.*, 1980). There is one important difference between the old and new maps; the earlier map showed two constitutive mutations at the leftmost end of *hisO*. We have mapped one of these mutations, *hisO3155*, and find it to lie in the attenuator region of *hisO*. The basis for this difference between our map and that of Ely *et al.* (1974) is unclear, but could reflect difficulties inherent in mapping particular alleles by three-point crosses. We feel that the deletion mapping used here is more reliable for fine-structure mapping of small regions of the chromosome.

We thank John Atkins for helpful discussions and for a critical reading of the manuscript. This work was supported by National Institutes of Health grant GM23408.

REFERENCES

Ames, B. N., Hartman, P. E. & Jacob, F. (1963). *J. Mol. Biol.* **7**, 23–42.
Artz, S. W. & Broach, J. R. (1975). *Proc. Nat. Acad. Sci., U.S.A.* **72**, 3453–3457.
Barnes, W. B. (1978). *Proc. Nat. Acad. Sci., U.S.A.* **75**, 4281–4285.
Bossi, L. & Cortese, R. (1977). *Nucl. Acids Res.* **4**, 1954–1956.
Bossi, L. & Roth, J. R. (1980). *Nature (London)*, **286**, 123–127.
Brenchley, J. E. & Ingraham, J. L. (1973). *J. Bacteriol.* **114**, 528–536.
Brenner, M. & Ames, B. N. (1971). In *Metabolic Pathways* (Greenberg, D. M. & Vogel, H. J., eds), vol. 5, Academic Press, New York.
Chang, G. W., Straus, D. & Ames, B. N. (1971). *J. Bacteriol.* **107**, 578–579.
Chumley, F. G. & Roth, J. R. (1980). *J. Mol. Biol.* **145**, 697–712.
Chumley, F. G., Menzel, R. & Roth, J. R. (1979). *Genetics*, **91**, 639–655.
DiNocera, P. P., Blasi, F., DiLauro, R., Frunzio, R. & Bruni, C. B. (1978). *Proc. Nat. Acad. Sci., U.S.A.* **75**, 4276–4280.
Ely, B. (1974). *Genetics*, **78**, 593–606.
Ely, B. & Ciesla, Z. (1974). *J. Bacteriol.* **120**, 984–986.
Ely, B., Fankhauser, D. B. & Hartman, P. E. (1974). *Genetics*, **78**, 607–631.
Fink, G. R. & Roth, J. R. (1968). *J. Mol. Biol.* **33**, 547–557.
Fink, G. R., Klopotowski, T. & Ames, B. N. (1967). *J. Mol. Biol.* **30**, 81–95.
Gorini, L. (1971). In *Ribosomes* (Nomura, M., Tissieres, A. & Lengyel, P., eds), pp. 791–803, Cold Spring Harbor Laboratories, New York.
Hartman, P. E., Hartman, Z., Stahl, R. C. & Ames, B. N. (1971). *Advan. Genet.* **16**, 1–56.
Hilton, J. L., Kearney, P. C. & Ames, B. N. (1965). *Arch. Biochem. Biophys.* **112**, 544–547.
Hoppe, I., Johnston, H. M., Biek, D. & Roth, J. R. (1979). *Genetics*, **92**, 17–26.
Ippen, K., Miller, J. H., Scaife, J. G. & Beckwith, J. R. (1968). *Nature (London)*, **217**, 825–827.
Jacob, F. & Monod, J. (1961). *J. Mol. Biol.* **3**, 318–356.
Johnston, H. M. & Roth, J. R. (1979). *Genetics*, **92**, 1–15.
Johnston, H. M. & Roth, J. R. (1980). *J. Mol. Biol.* **145**, 735–756.
Johnson, H. M., Barnes, W. M., Chumley, F. C., Bossi, L. & Roth, J. R. (1980). *Proc. Nat. Acad. Sci., U.S.A.* **77**, 508–512.
Kasai, T. (1974). *Nature (London)*, **219**, 523–527.
Keller, E. B. & Calvo, J. M. (1979). *Proc. Nat. Acad. Sci., U.S.A.* **76**, 6186–6190.
Kleckner, N. K., Roth, J. R. & Botstein, D. (1977). *J. Mol. Biol.* **116**, 125–159.
Martin, R. F., Berberich, M. A., Ames, B. N., Davis, W. W., Goldberger, R. F. & Yourno, J. D. (1971). *Methods Enzymol.* **17**, 3–34.
Murray, M. L. & Hartman, P. E. (1972). *Can. J. Microbiol.* **18**, 671–681.
Oxender, D. L., Zurawski, G. & Yanofsky, C. (1979). *Proc. Nat. Acad. Sci., U.S.A.* **76**, 5524–5528.
Roth, J. R. & Ames, B. N. (1966). *J. Mol. Biol.* **22**, 325–334.
Roth, J. R., Anton, D. N. & Hartman, P. E. (1966). *J. Mol. Biol.* **22**, 305–323.
Scott, J. F., Roth, J. R. & Artz, S. W. (1975). *Proc. Nat. Acad. Sci., U.S.A.* **72**, 5021–5025.
Silbert, B. F., Fink, G. R. & Ames, B. N. (1966). *J. Mol. Biol.* **22**, 335–347.
Singer, C. E., Smith, G. R., Cortese, R. & Ames, B. N. (1972). *Nature New Biol.* **238**, 71–73.
Voll, M. J. (1967). *J. Mol. Biol.* **30**, 109–124.
Winston, F., Botstein, D. & Miller, J. H. (1979). *J. Bacteriol.* **137**, 433–439.